

Interpreting Imagined Speech Waves with Machine Learning techniques

Abhiram Singh · Ashwin Gumaste

the date of receipt and acceptance should be inserted later

Abstract This work explores the possibility of decoding Imagined Speech (IS) signals which can be used to create a new design of Human-Computer Interface (HCI). Since the underlying process generating EEG signals is unknown, various feature extraction methods, along with different neural network (NN) models, are used to approximate data distribution and classify IS signals. Based on the experimental results, feed-forward NN model with ensemble and covariance matrix transformed features showed the highest performance in comparison to other existing methods. For comparison, three publicly available datasets were used. We report a mean classification accuracy of 80% between rest and imagined state, 96% and 80% for decoding long and short words on two datasets. These results show that it is possible to differentiate brain signals (generated during rest state) from the IS brain signals. Based on the experimental results, we suggest that the word length and complexity can be used to decode IS signals with high accuracy, and a BCI system can be designed with IS signals for computer interaction. These ideas, and results give direction for the development of a commercial level IS based BCI system, which can be used for human-computer interaction in daily life.

Keywords Brain-Computer Interface · Imagined Speech · Neural Networks · Tangent Space

1 Introduction

Brain-Machine Interface (BMI) is a collection of software (for analyzing cognitive tasks) and hardware components (used to capture brain signals). Nowadays, BMI research

is gaining momentum to diagnose brain disease, its possible use in human-computer interface (HCI) devices, and to study human behavior. When used as an HCI device, a BCI system can evolve with computer interaction technologies such as a keyboard, touch screen, or mouse. There exist many BMI systems for Human-Computer Interaction (HCI) [31] such as motor imaginary or P300.

A known fact about the human brain is that it generates electrical signals while performing different activities. One such class of brain signals is Imagined speech (IS) [12]. In IS condition, a person speaks in mind without moving any articulators. Note that the silent speech signals are different from IS, in which a user thinks about the articulator's movement for pronunciation of words. Previous studies suggest that the source of IS signals are Broca's and Wernicke's area [25], whereas the motor cortex of the brain is considered a primary source of silent speech signals.

With improvement in the technology, there exists different techniques to record electrical signals of the brain. Electroencephalography (EEG) [27] is one such non-invasive system, that involves placing electrodes over the scalp. EEG electrodes capture voltage differences generated due to ions movement inside the brain region. The voltage differences are captured and stored for a time duration to generate an EEG signal. The number of electrodes (1-256) are selected based on the experiment requirements.

The objective of this work is to explore different techniques that improve decoding capability of IS signals. A motivation to work on IS signals is to reduce the training time of participants and provide a more comfortable procedure for HCI than the motor imaginary tasks. Also, IS based BMI system offers a natural way towards HCI, which can lead to improved user experience in computer interaction. One assumption for the IS system to work is that the data is not fully corrupted. Therefore it is possible to extract IS speech

related information. Subjects participating in IS experiments follow specific guidelines to make this assumption feasible.

The work presented in this paper identifies a classification model and useful discriminative features to improve decoding performance on IS signals. Based on the experimental results on different datasets, Tangent Space (TS) [1] turns out to be the most discriminative input feature to an Artificial Feed Forward Neural Networks (ANN) [9] model. Our approach of TS+ANN improves the classification accuracy from 72.6% to 79.3%, 49.3% to 60.16%, and 49.2% to 57.83% on one long vs. short word, three short words and three vowels classification tasks respectively.

The following sections of this paper are as follows. Section 2 introduces the problem statement, and our contribution, along with an overview of existing methods to decode IS signals. Section 3 describes various classification models and feature extraction methods. Section 4 provides dataset detail and shows the result on different classification models in combination with appropriate feature extraction methods. Finally, section 5 discusses a few points for decoding IS signals and concluding remarks.

2 Problem Statement and Literature Review

In this section, we formally describe problem statement, our contributions and prior related work.

2.1 Problem Statement and Contribution

Problem Statement: For a given EEG signal, our goal is to identify signal category (imagined speech or other kind of brain signal). If signal belongs to the IS category, then we want to 1) decode word category; 2) actual imagined word.

Contribution: 1) We evaluate the generalization performance of neural networks (NN) on raw IS EEG signals. We show experimentally that for the given raw EEG signals of IS, the NN models fail to generalize. This leads us to the further exploration of various feature extraction techniques that are likely to improve NN performance. Main result: we identify Tangent Space [2] as the most useful discriminative feature and feed-forward NN as the most successful classification model for decoding IS. Results confirm that feature engineering indeed improved classifier performance. NN classifier performance was further improved by using an ensemble technique. Using experimental results, we also show that the presence of high-frequency components in an IS signals is required for enhancing the classifier performance. We compare and show results on three publicly available IS datasets and our approach outperformed existing approaches on different IS tasks. 2) We show that the feature extraction method used to decode IS signals is

also capable of discriminating participant's rest state EEG signals from the IS signals.

2.2 Related work

Zhao et al. [33] suggested support vector machines (SVM) with two different kernels and deep-belief networks (DBN) as classification models. The authors in [33] show results for each subject imagining some word or a phoneme. However, there are only about 10-15 trials per subject per word/phoneme. Hence, the classification result shown is on the limited amount of data and, therefore, does not have significant statistical importance. Rather than showing results for individual subjects, we have combined data of different subjects to obtain about 170 trials for each class (word/phoneme). This data was then used to compare the performance of different learning models. Suitability of the provided dataset lies in the fact that the data is of good spatial and temporal resolution.

Nguyen et al. [22] created three IS tasks comprising 2 long words, 3 short words and 3 vowels. Authors suggested covariance matrix based features (projected in Tangent Space (TS)) along with Relevance Vector Machine (RVM) [24] to decode IS signals. Results (in [22]) show the classification accuracy of 49%, 50% and 66% for vowels, short words, and long words respectively. We significantly improve these results by using TS features with principal component analysis (PCA) [15] to reduce feature dimensionality as well as use NN models for classification and ensemble techniques to improve model performance.

3 Proposed Approach for Imagined Speech Decoding

Our proposed approach for decoding the IS signal is summarized in the following steps. First, we attempt to decode raw EEG signals by feeding the signal directly as an input to different NN models. Raw EEG input will enable automatic feature extraction from the NN models leading to the learning of target class distribution. Second, we start exploring different feature extraction methods. For each feature extraction method, we select a classification model to represent temporal or spatial dependency among features. Third, we compare the performance of feature extraction, and associated classification models with the best IS decoding model. The above steps give us a comparative analysis of different features and classification models in the domain of IS signals. Finally, we compare our proposed approach with existing approaches for decoding IS signals.

3.1 Background on Classification Models

We now briefly describe the three NN models that are used for feature transformation and estimation of input condi-

tioned target class distribution. The parameters of all models were updated using the Adam optimization algorithm [16]. Gradient computation was performed with respect to the cross-entropy loss, and gradient propagation was performed using back-propagation.

The Artificial Neural Network (ANN) model [9] performs two steps in an iterative fashion: 1. linearly combine the output of previous hidden layer. 2. apply a non-linear activation function to generate the desired output:

$$a^l = g^l(M^l a^{l-1}) \quad (1)$$

Where, vector $a^{l-1} \in \mathbb{R}^n$ represents activations from the previous layer $l-1$, $a^l \in \mathbb{R}^m$ represents activations of layer l , weight matrix $M^l \in \mathbb{R}^{m \times n}$ contains tunable parameters between layer $l-1$ and l , and g^l is the ReLU activation function at the hidden layer l .

To capture dependency between inputs, some nodes in the network can have self-loops. This allows nodes to propagate the information across multiple inputs. The following relations govern the Recurrent Neural Network (RNN) [9]:

$$h^{(i)} = g(W_{hh}h^{(i-1)} + W_{hi}f^{(i)}); t_{pred}^{(i)} = g(W_{oh}h^{(i)}) \quad (2)$$

Where $f^{(i)} \in \mathbb{R}^n$ is the input, $t_{pred}^{(i)} \in \mathbb{R}^m$ is output, $h^{(i)} \in \mathbb{R}^k$ is hidden layer, $W_{hi} \in \mathbb{R}^{k \times n}$ is the weight matrix between input to hidden layer, $W_{hh} \in \mathbb{R}^{k \times k}$ is the weight matrix connecting hidden layer nodes to other hidden layer nodes, $W_{oh} \in \mathbb{R}^{m \times k}$ represents a kernel matrix from hidden to output layer, g is usually non-linear activation function.

In Convolutional Neural networks (CNN) [9] [32], a neuron is activated only for certain regions of a visual area known as a receptive field. Since neurons share parameters in one layer of the network and the receptive field dimension is much lower in comparison to an input dimension, the number of training parameters in CNN is much less than the number of parameters in the ANN for the same input dimension. A convolution operation is defined as the inner product between the weights of a layer (kernel/filter) and input neurons in the receptive field. This inner product is computed iteratively by shifting the window over the uncovered neurons. Some non-linear function and pooling layer usually follow the convolution layer. Feature map dimension after a convolution operation can be given as $1 + (n-k+2p)/s$. Where the input is of size $[n, n]$, while the kernel is of size $[k, k]$. The stride length is s , and padding size is p . We tried with different filter sizes to capture time and temporal dependency among EEG channels. To do so, we used max-pooling, a varied number of convolution and pooling layers, used ReLU and leaky-ReLU activation functions to improve overall model performance.

3.2 Approach

This section describes the various approaches that we took in decoding the IS signals.

Raw EEG signal + ANN: We start with raw EEG signals and use three different ANN models, (which are described in section 3.1) for feature extraction and estimation of conditional class distribution. Since ANN takes a vector as its input, the signal of each channel was appended along the time dimension to form a vector. For example, if a single EEG trial is of dimension $[c, t]$ where c and t represents the number of channels and samples in the trial, then a column vector of dimension $[t \times c, 1]$ was formed. A trial is a sequence of signal samples across different channels that corresponds to some cognitive activity. The limitation in this process is the high dimensionality of the input space in comparison to the available number of trials. This model has a large number of parameters to tune. Due to the limited size of the dataset, overfitting occurs in the early stage of learning.

Raw EEG signal + RNN: The next choice was the LSTM model [13], [9], which can capture time-dependency among input features. However, the high-sampling frequency of the EEG signal generated a long series of time-dependent signals. Despite down-sampling, it was not possible to reduce the sampling rate below 100 as most of the energy of the EEG signal is contained in the frequency band 0-50Hz. For a single EEG trial of $[c, t]$ dimension, a c -dimensional vector was given as input to LSTM for t time-steps. Out of the t outputs generated from LSTM, only the last output was used to identify the target class and measure cross-entropy loss.

Raw EEG signal + CNN: Next, we choose CNN because of its automatic feature extraction capabilities and successful application on a wide variety of EEG tasks [17]. The two dimensional EEG input of the form $[c, t]$ was given as input directly to the CNN to automatically extract features from raw EEG data and determine the appropriate target class.

Fourier Coefficients + ANN: We can also analyze the signal in another basis. The change of basis provides a different view and reveals the hidden properties of the signal. A change of basis might also serve as a dimension reduction technique, as the number of useful features can be reduced in another dimension. With this intuition, we start to explore a few signal transformation techniques. We can remove the time dependency by applying a signal transformation technique. In this case, the signal analysis was done in the Fourier domain (see [6] for details). The Fourier transformation (FT) provides a change of basis. Fourier coefficients are computed as:

$$Y[w] = \sum_{n=-\infty}^{\infty} y[n]e^{-iwn} \quad (3)$$

where, $y[n]$ is the discrete time signal, e^{-iwn} is the complex exponential at frequency, w and $Y[w]$ is the Fourier coefficient.

cient corresponding to the frequency w . Fourier coefficients representing frequency up to 40Hz were combined to form a vector. This Fourier coefficient vector was given as an input feature to the ANN model. FT was performed using Python Numpy library [29].

Spectrogram + CNN: By tracking frequency shifts with time, it might be possible to identify the effects of IS condition on the brain signals. To obtain both time and frequency representation of a signal, a spectrogram (see [26]) is used. The spectrogram is just stacking of frequency features over a time-axis, calculated using Short Time Fourier Transforms (STFT). The spectrogram was computed using the Python Scipy library [30]. For each channel of a trial, the spectrogram of dimension $[f, t]$ was calculated. By combining the spectrogram of each channel, we obtained data of dimension $[f, t, c]$, which was given as an input to a CNN, to track frequency shift with time along each channel. Where f is the number of frequency bins, t is the number of time bins, and c is the number of channels in an EEG trial.

Independent Components + CNN: The signal captured at EEG electrodes can be seen as a linear combination of signals generated due to a group of neuron activations and possibly due to some noise such as muscle artifact, eye movement, eye blinking, or environmental noise. During experiments, artifacts generated from the body are not present in all trials of a given target class, or even if they are present, then their presence will also be realized in other target classes. So the information provided by such artifacts in the experimental environment will not be useful in discriminating target classes for the given IS based EEG trials. Independent component analysis (ICA) [14] estimates the sources by assuming that source signals are linearly combined to generate observed signals, and source generating processes are independent of each other. The fastICA package [14], [23] was used to find independent components of brain signals, and these new components were given as $[c, t]$ - dimensional input to CNN.

Spatial Patterns + ANN: Common Spatial Pattern (CSP) [4] transforms the signals such that the variance of the signal is different for different classes. We can use the variance of each channel as an input feature to the classification model. Due to the use of target class information in features transformation step, this method is expected to improve classifier performance in comparison to the unsupervised features transformation techniques. CSP performs linear transformation as follows:

$$y^{new} = Ly \quad (4)$$

Where $y \in \mathbb{R}^n$, $y^{new} \in \mathbb{R}^n$ and transformation matrix $L \in \mathbb{R}^{n \times n}$. In the above, the classification performance gets improved by using y^{new} in comparison to y . For a two-class problem,

CSP can be seen as an optimization problem:

$$l^* = \underset{l \in \mathbb{R}^n}{\operatorname{argmax}} \left(\frac{l^T A_{y|c_1} l}{l^T A_{y|c_2} l} \right) \quad (5)$$

Where $l \in \mathbb{R}^n$ is the transformation vector, $A_{y|c_1}$ and $A_{y|c_2} \in \mathbb{R}^{n \times n}$ are the covariance matrix of data belonging to class 1 and 2, l^* is the optimized transformation vector. For dimension reduction, transformation matrix $L \in \mathbb{R}^{j \times n}$ with $j < n$ can be used. Solution to optimization problem in equation 5 can be obtained by solving the following problem:

$$A_{y|c_1} l = \omega A_{y|c_2} l \quad (6)$$

where ω is the eigenvalue and l is corresponding eigenvector. After transformation of EEG signals according to equation 4 (CSP package [10]), the variance of each channel is calculated to form a c -dimensional vector and given as an input feature to the ANN.

Tangent Space + ANN: For a given EEG trial, it is possible to measure the spatial dependency between EEG channels by computing the covariance matrix. The covariance matrices must be represented in a vector form to apply various dimension reduction techniques. However, the projection must preserve the discriminative information of the target class. To this end, covariance matrices are projected to the tangent space (TS) [1] involving the following matrix operations:

$$P_i = C_m^{1/2} \log m(C_m^{-1/2} C_i C_m^{-1/2}) C_m^{1/2} \quad (7)$$

$$\log m(N) = AB^T A^{-1}, B^T[i, i] = \log(B[i, i])$$

Where C_i is an input covariance matrix, C_m represents the mean of covariance matrices, P_i is the required projection, N is a diagonalizable matrix, N^{-1} is the matrix inverse, and ABA^{-1} is the decomposition of the matrix N . Same decomposition ABA^{-1} of matrix N can be used to compute $N^{-1/2}$. The final transformation step flattens the matrix P_i to obtain a vector representation. The dimension of flattened vector is reduced using Principal Component Analysis (PCA) [15] and then given as an input to the ANN. Computation of tangent vectors was performed using the Pyriemann library [3].

Bagging + ANN: We used the Bootstrap Aggregation (Bagging) Classifier [5] with ANN as its base classifier. Bagging classifier trains multiple base classifiers on a small random subsets of the dataset. The result of each base classifier is combined by averaging, which provides a single output of the Bagging classifier. Bagging improves mean classification accuracy and reduces the variance of the base classifier. We used a bagging classifier for the ANN classifier only. Training of CNN and LSTM is computationally intensive, and hence bagging was not used with these classifiers.

3.3 Data Visualization

For data visualization in two dimensions, we use PCA and tSNE [18]. The objective function of PCA is,

$$\begin{aligned} & \max_{u \in \mathbb{R}^n} u^T A u \\ & \text{subject to } \|u\|_2^2 = 1 \end{aligned} \quad (8)$$

Here, A is the data covariance matrix defined as $\frac{1}{m} \sum_{i=1}^m x^{(i)} x^{(i)T}$ and $u, x^{(i)} \in \mathbb{R}^n$. The optimization problem (defined in equation 8) can be solved by obtaining a solution to the Eigenvalue problem $Au = \omega u$.

The t-distributed stochastic neighbor embedding (t-SNE) computes probabilities by using the distance between points as a measure. The computed probabilities define distribution in a higher and lower dimension. The difference between these two distributions is minimized by using Kullback-Leibler (KL) divergence as a cost function. KL divergence is defined as,

$$KL(P, Q) = \sum_{i \neq j} p_{ij} \log \frac{p_{ij}}{q_{ij}} \quad (9)$$

Where P, Q are two distributions defined in higher and lower dimensions, respectively. t-SNE implementation [22] was used for dimension reduction.

4 Dataset Details and Results

Now we discuss the datasets in detail, explain various pre-processing steps, show the performance of our proposed approach on these datasets, and finally compare obtained results with existing approaches.

4.1 Dataset details and Pre-processing

We use three publicly available datasets given by Zhao et al. [33], Nguyen et al. [22] and Coretto et al. [7], which we shall term as *dataset1*, *dataset2* and *dataset3* respectively. *Dataset1* contains 11 categories (*iy, uw, piy, tiy, diy, m, n, pat, pot, knew, gnaw*) from 13 subjects. We call EEG data corresponding to an output label, a trial. We reject a few trials because these contain relatively high or low values, possibly due to some error in the experiments. The remaining 1735 trials were low-pass filtered with an upper cut-off frequency of 40Hz. After that, each trial was down-sampled to 128Hz from 1000Hz. We restrict the number of samples in each trial to 619 to remove variation across trials. Finally, trials corresponding to each output class were appended sequentially to form a 3D matrix of dimension [1735, 62, 619] and targets of each category as one hot 11-dimensional vector.

Dataset2 contains eight categories (*a, i, u, in, out, up, independent, cooperate*) with three subcategories having three vowels, three short words and two long words. Each category contains 100 trials per subject. For vowels and short words, the trial duration was of 1 second, and for long words, the trial duration was 1.4 seconds. The dataset was down-sampled to 256Hz. In a trial, subjects performed three repetitive thinking of the same word or vowel. Therefore each trial provides three matrices of $[c, t]$ dimension. For long words matrix dimension is [60, 360] and for vowels and short words matrix dimension is [60, 256]. Therefore, we have [600, 60, 360] or [900, 60, 256] dimensional data matrix for each subject and 2 or 3-dimensional one-hot vector representation as target classes.

Dataset3 contains 11 categories (*a, e, i, o, u, up, down, left, right, backward, forward*) with data collected from 15 subjects. Each vowel or word has approximately 50 trials repeated in random order by each subject. However, only six electrodes are used in the experiment and the sampling frequency is 1024Hz. In each trial, the imagined speech duration was set to 4 seconds following the rest state condition, which was for another 4 seconds. Data of each subject was stored in the format $[N, C, T]$ where N is the number of trials for any subject, C is the number of channels, and T is the number of samples in that trial. In our case, if a subject is having exactly 50 trials for each category then, the input is a [550, 6, 4096] dimensional matrix and 11 or 2-dimensional one-hot vector (depending on the decoding of all categories simultaneously or decoding vowels vs. words) as the target. Data in the above format was taken as processed input to different methods, and then we performed feature transformation and decoding (as described in section 3).

4.2 Results

In this section, different feature extraction methods and classification models are evaluated for decoding IS signals.

4.2.1 Performance metric

Classification accuracy (CA) is used as a metric to compare the performance of different approaches. CA calculates the fraction between the number of correct predictions vs. total predictions. Accuracy results are reported using the 10-fold cross-validation scheme. Each fold involves data separation (using the stratified sampling) into a train and test set. Stratified sampling maintains the sample proportion of each class in the train and test sets.

4.2.2 Results on dataset1

We follow an incremental approach in which, based on initial stage results, we select only top-performing feature ex-

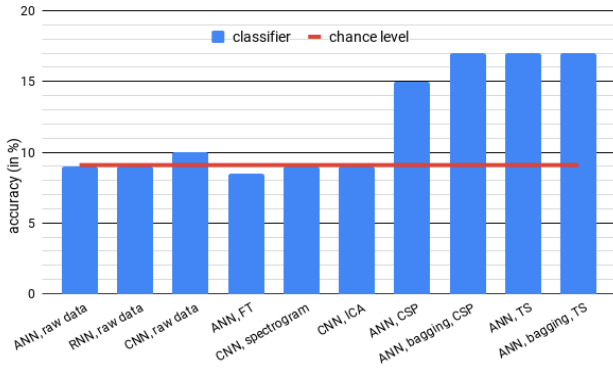


Fig. 1: 11 class classification on *dataset1*.

traction methods and related models. We start evaluating the performance of different feature extraction and classification models with *dataset1*. The results are shown in Figure 1 where each column shows accuracy after decoding 11 categories of the IS based EEG signal. From Figure 1, it is clear that CSP and TS feature extraction methods outperform other methods. Bagging also slightly helps in the performance improvement. Other feature extraction methods (described in section 3) do not generalize to the classification task, and hence we report further results on *dataset2* and *dataset3* using CSP and TS based methods. Using TS and CSP, we also checked individual performance for seven phonemes and four words, as shown in Figure 2. Here, both methods gave slightly improved results when compared to the chance level accuracy. Chance level accuracy in seven phonemes and four words task is 14.28% and 25%, respectively.

Subsequently, we checked whether it is possible to discriminate between words based on their length. We combined trials of words and phonemes in two different groups and applied CSP and TS methods with ANN. In this case, we obtained high accuracy (Figure 2). CSP+ANN showed 94% accuracy, and TS+ANN showed 96% accuracy. Bagging slightly improved performance in both cases. Chance level accuracy in the word-vs-phoneme classification task is 50%.

It is pertinent to note that in Figure 2, we compared results by combining the data of all the subjects. This requirement came from the fact that there are only about 10-15 trials per subject per class. Model learning and performance comparison cannot be done on very few training and testing examples. Combining data of different subjects might hurt the model performance, but it increased the number of training examples to about ten times (for each target class). Increased number of training samples helped us in identifying the best feature extraction method and model for the IS recognition task.

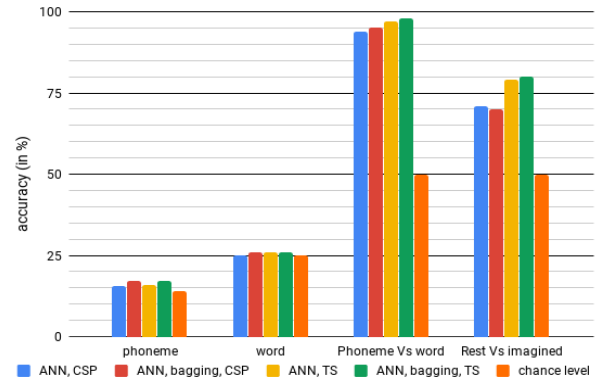


Fig. 2: Classification on four different tasks of *dataset1*.

Rest vs. IS state: To develop a real-time IS based BCI system, it is necessary to distinguish between IS and rest-state conditions. For classifying IS signal from rest-state brain signal, we extracted rest-state EEG signals from the available dataset and applied the same pre-processing steps as for the case of imagined speech signals. Then trials corresponding to imagined speech signals and rest state signals were divided into two different groups to form a binary classification problem. We applied CSP+ANN and TS+ANN models to solve binary classification problem. Using CSP features, 71% accuracy, and using TS features, 79% accuracy was obtained (Figure 2). These results confirm that IS EEG signals carry a lot of discriminative information from brain signals generated during the rest-state.

Dataset1 visualization: Results on *dataset1* show very low accuracy on the multiclass problem and high accuracy on binary classification. This point is worth investigation, and we understand this behavior by visualization of points in lower dimensions (see Figure 3). For this, we used the TS features and projected these to 2 dimensions using PCA and tSNE. Projected points are plotted with different colors, with each color representing the target class for that point.

As we can see from Figure 3, the points for the multiclass problem are mixed up heavily. PCA tends to form 5 to 6 clusters and each cluster has data from multiple classes. Hence it becomes difficult to find a clear separation boundary. In higher dimensions, points may be separated. However, classification results show that even in a higher dimension, a clear separation cannot be obtained with a good generalization capability. When observing data using tSNE, about 13-14 well-separated clusters are formed. However, data-points of different classes continue to be present within each cluster, which makes it difficult for a classifier to separate points. For binary classification using PCA, we can see that data of two classes is overlapping with a slight shift of points belonging to different classes. Using tSNE for binary classification between words and phonemes, the separation between points belonging to each cluster is more visible.

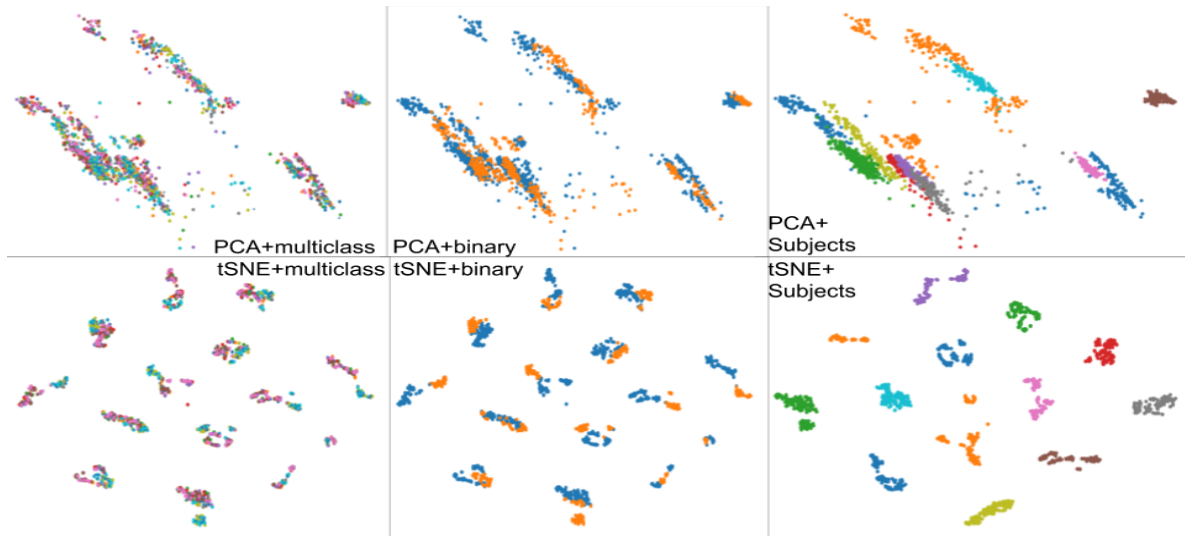


Fig. 3: TS in the lower dimension using PCA and tSNE for *dataset1*. Two figures on the left show data points for 11 target classes, and two figures in the middle show binary classification between words and phonemes. The rightmost figures show data points for each subject. Top figures are obtained using PCA and bottom are obtained using tSNE. Each color in the left and central figure represents a target class of that point, and each color in the rightmost figures belongs to different subjects. The rightmost figure using tSNE, shows one cluster per subject.

This visualization becomes more evident in higher dimensions as the classifier can create a separation boundary with good generalization performance on the test set.

By observing data in a lower dimension using the t-SNE approach, we can see some clusters. Counting of these clusters was approximately equal to the number of participants in the experiment. The next obvious question was to check if these clusters are indeed representing different participants. To this end, data of different participants was appended sequentially. TS based features were extracted, and then PCA and t-SNE on these features were applied and plotted for each subject (rightmost part of Fig 3). PCA and t-SNE both show clusters for each participant, but the division is visible only in the latter approach. This visualization clearly shows a possible application of the IS based EEG signals in the domain of biometric-based human authentication.

4.2.3 Results on dataset2

To further check the robustness of the proposed approach, the performance of these methods was compared on *dataset2*. Due to availability of data-points, we show results for each subject, by training and testing on individual subjects' data. Figure 4 shows results for 3 short words, 2 long words, 3 vowels, and 1 short vs. long word, respectively. A comparison of CSP+ANN and TS+ANN is made with results provided Nguyen et al. [22] who proposed tangent space (TS) with Relevance Vector Machine (RVM). Our findings on *dataset1* clearly show that Bagging gave improved results. To this end, we used CSP+ANN and TS+ANN with Bagging

for comparing results with the TS+RVM approach. We can see that the TS+RVM approach dominates over the CSP approach, but our proposed approach of using TS+ANN+ Bagging outperformed TS+RVM approach on 3 vowels (Figure 4c) and 3 short words (Figure 4a) classification tasks. Further, our approach performed equally well or better for many subjects on long vs. short words (Figure 4d) and 2 long words (Figure 4b) classification task. Note that chance level accuracy for 3 vowels and 3 short words classification is 33.33%, and for 2 long words and one short vs. long word classification is 50%.

Comparison with existing approaches: Now we compare four existing approaches of IS decoding with our proposed approach (TS+ANN+bagging). First, we compare our method with the approach suggested by Tomioka et al. [28], which applies CSP to the input data, calculates the log of the variance of each channel and uses linear discriminant analysis (LDA) as a classifier. The second comparison is made with Dasalla et al. [8], in which authors suggest using CSP based feature transformation technique with a support vector machine (SVM) classifier. The third comparison is made with Min et al. [20]. This approach uses mean, variance, standard deviation, and skewness as the input features to the extreme learning machine (ELM). The final comparison is made with Nguyen et al. [22] approach of using TS as input features to ELM. We have already shown the results of Nguyen et al. [22] method of using TS as an input feature to the RVM classifier (Figures 4). Figures 5 show the performance of four existing approaches with our proposed approach on one long vs. one short word, 3 short words, and

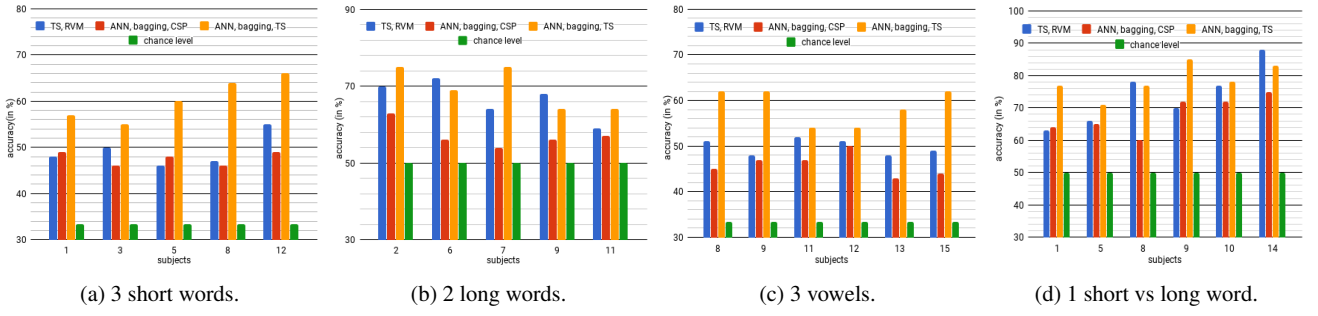


Fig. 4: Evaluation of the proposed approach (CSP and TS with ANN+bagging classifiers) on four different tasks of *dataset2* and comparison with TS+RVM approach.

3 vowels classification tasks, respectively. Our proposed approach of using TS+ANN+bagging outperformed all four existing approaches. This performance improvement is seen across all the subjects performing three different IS tasks.

From Figure 5, we observe the variation in the performance of each approach across different subjects. A more interpretable way for the comparison is to compute a single result for each approach. To this end, the accuracy of all subject within a task is averaged to obtain one performance measure. Table 1 shows the results for each task.

Table 1: Classification Accuracy (μ) And Standard Deviation (σ). Results are rounded to the nearest integer. N.A. stands for results not available in [22].

Task		Vowels	Short words	Short Vs. Long	Long words
lda+csp	μ	35	34	65	N.A.
	σ	4	7	10	N.A.
elm+ts	μ	45	47	75	N.A.
	σ	2	5	5	N.A.
svm+csp	μ	35	39	61	N.A.
	σ	4	3	5	N.A.
rvm+ts	μ	49	50	73	66
	σ	2	3	9	5
elm+statistical features	μ	37	43	56	N.A.
	σ	5	6	5	N.A.
ann+ts	μ	58	60	79	69
	σ	3	4	5	5

It is evident from Table 1 that the proposed approach (ts+ann) obtains the highest classification accuracy across different classification tasks. The low deviation of the proposed approach implies that ANN model with begging reduces the variability across subjects. A desired approach should provide high mean accuracy with low variance, where mean and variance is calculated across all subjects. Our approach appears to reach that point. Existing approaches for decoding IS signal either obtain high accuracy and high variance or low accuracy and low variance across different sub-

jects. This implies that existing approaches exhibits one of the following two cases: 1. Decode IS signals of only a few subjects with high accuracy, thereby showing high variance. 2. Unable to extract IS based discriminative information, thereby resulting low accuracy and small deviation.

Experimental results (presented in this paper) show the generalization capability of the ANN model in decoding IS signals when appropriate input features are provided. Note that the classification accuracy of words in the *dataset1* is much lower than *dataset2*. High accuracy on *dataset2* suggests that the word complexity and length provide useful discriminative information in IS word decoding tasks.

High-frequency component (HFC) analysis: From the work of Emily et al. [21], Martin et al. [19] and Herff et al. [11] (in which they used ElectroCortigoGraphy (ECoG) to measure IS based brain signals), it is quite evident that they mainly used signals with high-frequency components and thereby obtained good decoding results. However, due to the invasive nature of ECoG, it is not possible to use this technique, which is hence limited to medical patients. Despite this limitation, the ECoG motivates for checking whether we can use high-frequency components (HFCs) of EEG signals to improve decoding power. The common reason for not trying HFCs is because the signal strength drops rapidly with an increase in HFCs, and the SNR becomes low. Hence, it becomes difficult to separate signal from noise.

To study the importance of HFCs above 50Hz in IS based EEG signals, the data belonging to two long words as a classification task was band-pass filtered between 80 and 125Hz. After that, the TS based feature extraction technique was applied with ANN and bagging. Post-classification, the results were then compared with an unfiltered signal and a 40Hz low-pass filtered signal belonging to the same two long words task. Figure 6 shows slight performance improvement as compared to the unfiltered signal. The lowest performance was obtained when classifying the 40Hz low-pass filtered signal. We can see up to 5% difference in accuracy between the HFCs signal and low-pass signal for up to 40Hz. These results were consistent for all the subjects.

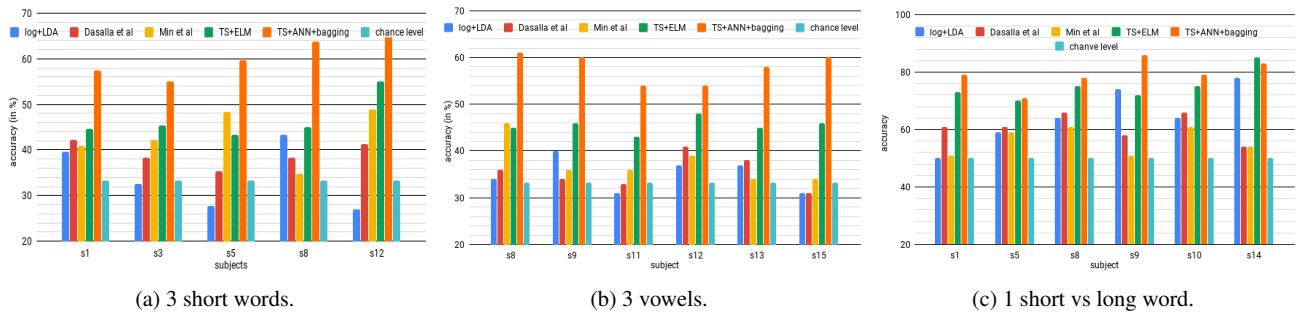


Fig. 5: Comparison of the proposed approach (ts+ANN+bagging) with existing approaches on three IS tasks of *dataset2*.

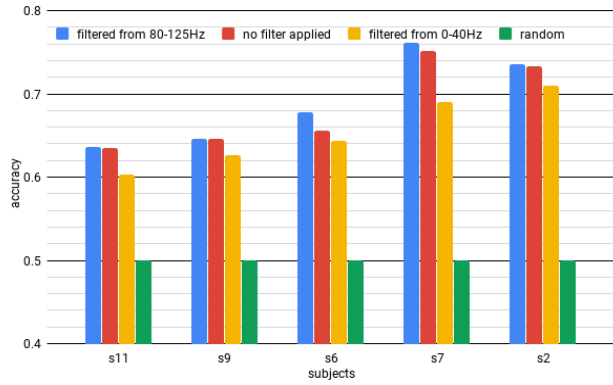


Fig. 6: Using the band-pass filtered signal for two long words classification task on *dataset2*.

Table 2: Hyper-parameter setting and model accuracy for two long words classification task on *dataset2*.

Subjects	s11	s9	s6	s7	s2
Neurons	100	200	50	150	50
Estimators	100	200	100	10	50
Dimensions	20	70	20	20	20

The usual trend in EEG signal processing is to apply a low-pass filter up to 40Hz and then extract information from the filtered signal. This result clearly shows that even if the signal amplitude is much lower for HFCs, the discriminative information continues to be present in those components. Hence low-pass filtering of IS based EEG signals is not always the right choice.

Hyper-parameter details: Now, we provide hyperparameter details on a 2 long words classification task applied on *dataset2* (Table 2). We used ANN with one hidden layer and a table row called neurons that denotes the number of neurons in the hidden layer. Bagging requires that the number of classifiers to be specified (estimators row in Table 2). We have 60 EEG channels in *dataset2*, implying that the length of the tangent vector was 1830. For dimension reduction, we used PCA. In Table 2, the row named dimensions specifies the number of components retained after applying PCA.

4.2.4 Results on dataset3

With the above setting, we applied our method to *dataset3* [7] in which six electrodes were used to capture EEG signals during the IS recognition task.

We show results for eleven and binary classification in Table 3. The length of the feature vector after transformation was 21. So, after applying TS, there was no need to reduce the dimension. This feature vector was directly given as an input to the bagging classifier, which uses ANN as a base classifier.

Due to the imbalance of data in *dataset3* for the binary classification task, along with classification accuracy, we also report the area under the curve (AUC) in the result. AUC measures an area under the Receiver Operating Characteristic (ROC) curve. The ROC curve is plotted by measuring the true-positive rate (TPR) and false-positive rate (FPR) of the classifier for different values of threshold. An AUC of 0.5 shows random performance from the classifier. On the other hand, an AUC value of 1 implies that the classifier can correctly separate the classes. Hence, we want a classifier with a higher AUC value. Table 3 shows classification accuracy and AUC for different subjects. The chance level accuracy for binary classification between vowels, and words is 0.5 and that for 11 class classification is 0.0909.

We observe low accuracy in multiclass categorization, as well as in binary classification. The reason for this observation is the reduced number of electrodes, which reduces the presence of useful discriminative information in the data. Also, the signal was low-pass filtered up to 40Hz, which drops the classifier performance (as shown in the result of *dataset2*). Another reason is the choice of words based on their meaning. We have seen from results on *dataset1* and *dataset2* that the word complexity is useful discriminative information, and it also helps in improving classifier performance. It is clear that words in *dataset3* are not complex (in terms of their speech representation), and hence their decoding is more difficult even in the binary classification task.

Table 3: Subjects performance on vowels vs words (binary) and 11 (multi) class classification task on *dataset3*. accBinary and aucBinary represents model accuracy and AUC for Binary classification task, accMulti and aucMulti represents multiclass classification task.

Subjects	s13	s3	s11	s14	s1
accBinary	0.669	0.678	0.685	0.685	0.626
aucBinary	0.662	0.671	0.677	0.681	0.625
accMulti	0.117	0.147	0.114	0.114	0.125
aucMulti	0.536	0.582	0.552	0.551	0.555
Subjects	s6	s5	s7	s15	s8
accBinary	0.719	0.591	0.572	0.632	0.766
aucBinary	0.721	0.586	0.555	0.627	0.76
accMulti	0.109	0.103	0.097	0.144	0.127
aucMulti	0.565	0.505	0.488	0.559	0.624
Subjects	s4	s12	s10	s9	s2
accBinary	0.572	0.559	0.65	0.651	0.661
aucBinary	0.561	0.549	0.643	0.649	0.605
accMulti	0.113	0.135	0.12	0.111	0.118
aucMulti	0.545	0.542	0.54	0.563	0.543

5 Discussion and Conclusion

In this section, we provide some reasoning behind the variation of model performance across three datasets and after that we provide concluding remarks.

5.1 Discussion

We see the highest multiclass classification performance on *dataset2*, highest binary classification on *dataset1* and least performance on *dataset3*. On *dataset2*, multiclass classification accuracy is high (as compared to the other datasets) because words or vowels differ in their speech signal representation. Therefore a process generating these speech signals possibly activates the neurons at different time intervals to generate activation patterns. Different activation patterns lead to the discriminative IS based EEG signals. Generally, long words are more difficult in the imagined speech pronunciation in comparison to the vowels and short words. This additive complexity contained in the IS signals provides more discriminative information, thereby improving the classifier performance.

For *dataset1*, we see similar phonemes and words. Hence, during the imagination of similar kinds of words, internal brain representation might be related. Therefore, we observe low performance using multiclass classification tasks. But the same phonemes and words can be grouped to provide substantial discriminative information giving good accuracy for binary classification tasks between phonemes and words. High accuracy on binary classification task shows that the brain has a similar representation for words that sound similar to each other. This result also holds for binary categorization of vowels and words. The accuracy is lower in *dataset3*,

but this is primarily due to using very few electrodes and low-pass signal filtering. Multiclass results are also low because of the similar reasons. One additional point for low accuracy in *dataset3* is that words were chosen based on different meanings rather than selecting words based on the difference in their sound, length, and complexity.

5.2 Conclusion

The work presented in this paper shows a technique to design and develop an imagined speech based BMI system with the help of machine learning techniques. In doing so, we explored various feature engineering methods and different neural network models to understand the decoding capability of IS signals. Subsequently, we proposed an approach (TS+PCA+ANN+bagging) that gives the best result among different explored methods. The proposed approach outperformed existing methods when applied to three publicly available datasets. We show that IS signals contain some information that can be used when differentiating IS signals from other brain signals. We also suggest that the length and complexity of a word are a useful criterion while discriminating against a group of words. The future work will be dedicated on creating a machine learning model that can directly decode raw EEG signals and can recover from noisy signals.

References

1. Barachant, A., Bonnet, S., Congedo, M., Jutten, C.: Multiclass brain-computer interface classification by riemannian geometry. *IEEE Transactions on Biomedical Engineering* **59**(4), 920–928 (2012). DOI 10.1109/TBME.2011.2172210
2. Barachant, A., Bonnet, S., Congedo, M., Jutten, C.: Classification of covariance matrices using a riemannian-based kernel for bci applications. *Neurocomputing* **112**, 172 – 178 (2013). DOI <https://doi.org/10.1016/j.neucom.2012.12.039>. URL <http://www.sciencedirect.com/science/article/pii/S0925231213001574>. Advances in artificial neural networks, machine learning, and computational intelligence
3. Barachant, A., et al.: pyriemann: Biosignals classification with riemannian geometry (2015). URL <https://github.com/alexandrebarachant/pyRiemann>. Library available from <http://pyriemann.readthedocs.io/en/latest/index.html>
4. Blankertz, B., Tomioka, R., Lemm, S., Kawanabe, M., r. Muller, K.: Optimizing spatial filters for robust eeg single-trial analysis. *IEEE Signal Processing Magazine* **25**(1), 41–56 (2008). DOI 10.1109/MSP.2008.4408441
5. Breiman, L.: Bagging predictors. *Machine Learning* **24**(2), 123–140 (1996). DOI 10.1007/BF00058655. URL <https://doi.org/10.1007/BF00058655>
6. Cooley, J.W., Tukey, J.W.: An Algorithm for the Machine Calculation of Complex Fourier Series. *Math. Comput.* **19**, 297–301 (1965). DOI 10.1090/S0025-5718-1965-0178586-1
7. Coretto, G., Gareis, I., Rufiner, H.: Open access database of eeg signals recorded during imagined speech. p. 1016002 (2017). DOI 10.1117/12.2255697

8. DaSalla, C.S., Kambara, H., Sato, M., Koike, Y.: Single-trial classification of vowel speech imagery using common spatial patterns. *Neural Networks* **22**(9), 1334 – 1339 (2009). DOI <https://doi.org/10.1016/j.neunet.2009.05.008>. URL <http://www.sciencedirect.com/science/article/pii/S0893608009000999>. Brain-Machine Interface
9. Goodfellow, I., Bengio, Y., Courville, A.: *Deep Learning*. The MIT Press (2016)
10. Gramfort, A., Luessi, M., Larson, E., Engemann, D.A., Strohmeier, D., Brodbeck, C., Parkkonen, L., Hämäläinen, M.S.: Mne software for processing meg and eeg data. *NeuroImage* **86**, 446 – 460 (2014). DOI <https://doi.org/10.1016/j.neuroimage.2013.10.027>. URL <http://www.sciencedirect.com/science/article/pii/S1053811913010501>
11. Herff, C., Heger, D., De Pestiers, A., Telaar, D., Brunner, P., Schalk, G., Schultz, T.: Brain-to-text: Decoding spoken phrases from phone representations in the brain. *Frontiers in Neuroscience* **9** (2015). DOI 10.3389/fnins.2015.00217
12. Hickok, G., Poeppel, D.: The cortical organization of speech processing. *Nature Reviews Neuroscience* **8**, 393–402 (2007)
13. Hochreiter, S., Schmidhuber, J.: Long short-term memory. *Neural Comput.* **9**(8), 1735–1780 (1997). DOI 10.1162/neco.1997.9.8.1735. URL <https://doi.org/10.1162/neco.1997.9.8.1735>
14. Hyvärinen, A., Oja, E.: Independent component analysis: Algorithms and applications. *Neural Netw.* **13**(4–5), 411–430 (2000). DOI 10.1016/S0893-6080(00)00026-5. URL [https://doi.org/10.1016/S0893-6080\(00\)00026-5](https://doi.org/10.1016/S0893-6080(00)00026-5)
15. Jolliffe, I.: *Principal Component Analysis*. John Wiley & Sons, Ltd (2014). DOI 10.1002/9781118445112.stat06472. URL <http://dx.doi.org/10.1002/9781118445112.stat06472>
16. Kingma, D.P., Ba, J.: Adam: A method for stochastic optimization. *CoRR* **abs/1412.6980** (2014). URL <http://arxiv.org/abs/1412.6980>
17. Lawhern, V.J., Solon, A.J., Waytowich, N.R., Gordon, S.M., Hung, C.P., Lance, B.J.: Eegnet: A compact convolutional network for eeg-based brain-computer interfaces. *CoRR* **abs/1611.08024** (2016). URL <http://arxiv.org/abs/1611.08024>
18. van der Maaten, L., Hinton, G.: Visualizing high-dimensional data using t-sne. *Journal of Machine Learning Research* (2008)
19. Martin, S., Brunner, P., Iturrate, I., Millan, J.d.R., Schalk, G., Knight, R., Pasley, B.: Corrigendum: Word pair classification during imagined speech using direct brain recordings. *Scientific Reports* **7**, 44509 (2017). DOI 10.1038/srep44509
20. Min, B., Kim, J., Jun Park, H., Lee, B.: Vowel imagery decoding toward silent speech bci using extreme learning machine with electroencephalogram. In: *BioMed research international* (2016)
21. Mugler, E., Patton, J., Flint, R., Wright, Z., Schuele, S., Rosenow, J., Shih, J., Krusienski, D., Slutzky, M.: Direct classification of all american english phonemes using signals from functional speech motor cortex. *Journal of neural engineering* **11**, 035015 (2014). DOI 10.1088/1741-2560/11/3/035015
22. Nguyen, C.H., Karavas, G.K., Artemiadis, P.K.: Inferring imagined speech using eeg signals: a new approach using riemannian manifold features. *Journal of neural engineering* **15** **1**, 016002 (2018)
23. Pedregosa, F., Varoquaux, G., Gramfort, A., Michel, V., Thirion, B., Grisel, O., Blondel, M., Prettenhofer, P., Weiss, R., Dubourg, V., Vanderplas, J., Passos, A., Cournapeau, D., Brucher, M., Perrot, M., Duchesnay, E.: Scikit-learn: Machine learning in Python. *Journal of Machine Learning Research* **12**, 2825–2830 (2011)
24. Psorakis, I., Damoulas, T., Girolami, M.A.: Multiclass relevance vector machines: Sparsity and accuracy. *IEEE Transactions on Neural Networks* **21**(10), 1588–1598 (2010). DOI 10.1109/TNN.2010.2064787
25. Sahin, N.T., Pinker, S., Cash, S.S., Schomer, D.L., Halgren, E.: Sequential processing of lexical, grammatical, and phonological information within broca’s area. *Science* **326** **5951**, 445–9 (2009)
26. Sejdić, E., Djurović, I., Jiang, J.: Time–frequency feature representation using energy concentration: An overview of recent advances. *Digital Signal Processing* **19**(1), 153 – 183 (2009). DOI <https://doi.org/10.1016/j.dsp.2007.12.004>. URL <http://www.sciencedirect.com/science/article/pii/S105120040800002X>
27. Teplan, M.: Fundamental of eeg measurement. *MEASUREMENT SCIENCE REVIEW* **2** (2002)
28. Tomioka, R., Müller, K.R.: A regularized discriminative framework for eeg analysis with application to brain–computer interface. *NeuroImage* **49**(1), 415 – 432 (2010). DOI <https://doi.org/10.1016/j.neuroimage.2009.07.045>. URL <http://www.sciencedirect.com/science/article/pii/S1053811909008192>
29. van der Walt, S., Colbert, S.C., Varoquaux, G.: The numpy array: A structure for efficient numerical computation. *Computing in Science Engineering* **13**(2), 22–30 (2011)
30. Virtanen, P.e.a.: *SciPy 1.0: Fundamental Algorithms for Scientific Computing in Python*. *Nature Methods* **17**, 261–272 (2020). DOI <https://doi.org/10.1038/s41592-019-0686-2>
31. Wolpaw, J., Wolpaw, E.: *Brain-Computer Interfaces: Principles and Practice*. Oxford University Press, USA (2012). URL https://books.google.co.in/books?id=tC2UzuC_WBQC
32. Zeiler, M.D., Fergus, R.: Visualizing and understanding convolutional networks. *CoRR* **abs/1311.2901** (2013). URL <http://arxiv.org/abs/1311.2901>
33. Zhao, S., Rudzicz, F.: Classifying phonological categories in imagined and articulated speech. In: *2015 IEEE International Conference on Acoustics, Speech and Signal Processing (ICASSP)*, pp. 992–996 (2015)